Earthq Eng & Eng Vib (2022) 21: 987-998 **DOI**: https://doi.org/10.1007/s11803-022-2131-2

Simulation research on the energy dissipation and shock absorption performance of a swing column device based on fuzzy control

Zheng Yong[1,2,3†] and Yuan Bo[1,3‡]

1. *Research Center of Space Structures, Guizhou University, Guiyang 550004, China*
2. *College of Civil Engineering, Guizhou University, Guiyang 550004, China*
3. *Key Laboratory of Structural Engineering of Guizhou Province, Guiyang 550025, China*

Abstract: Double-column bridge piers are prone to local damage during earthquakes, leading to the destruction of bridges. To improve the earthquake resistance of double-column bridge piers, a novel swing column device (SCD), consisting of a magnetorheological (MR) damper, a current controller, and a swing column, was designed for the present work. To verify the seismic energy dissipation ability of the SCD, a lumped mass model for a double-column bridge pier with the SCD was established according to the low-order modeling method proposed by Steo. Furthermore, the motion equation of the double-column bridge pier with the SCD was established based on the D′Alembert principle and solved with the use of computational programming. It was found that the displacement response of the double-column bridge pier was effectively controlled by the SCD. However, due to rough current selection and a time delay, there is a significant overshoot of the bridge acceleration using SCD. Hence, to solve the overshoot phenomenon, a current controller was designed based on fuzzy logic theory. It was found that the SCD design based on fuzzy control provided an ideal shock absorption effect, while reducing the displacement and acceleration of the bridge pier by 36.43% – 40.63% and 30.06% – 33.6%, respectively.

Keywords: swing column device; double-column bridge pier; fuzzy control; MR damper; structural control; low-element modeling method

1 Introduction

Bridge structures play an important role in transportation (Panji *et al.*, 2017; Wang *et al.*, 2020); therefore, it is crucial to effectively control and mitigate their earthquake-induced vibration. A damping device, such as a magnetorheological (MR) damper, a viscous damper (VD), or a tuned mass damper (TMD), is generally installed to reduce the dynamic response of bridges (Huang *et al.*, 2019; Kahya and Araz, 2020; Lavasani *et al.*, 2020; Li *et al.*, 2020; Niu *et al.*, 2020; Pozos-Estrada *et al.*, 2011; Xu *et al.*, 2019; Zhao *et al.*, 2019). Semi-active MR dampers have significant advantages because of their good controllability, low energy consumption, fast response, and outstanding adaptability (Jiang and Christenson, 2012; Xu *et al.*, 2012). Therefore, they could be used as vibration controllers for bridge structures.

Bridge piers act as primary load-bearing elements of bridge structures and are prone to sever vibration due to their small transverse stiffness and natural damping. Hence, it is necessary to improve the seismic performance of bridge piers (Xie and Qu, 2018). Arsava *et al*. (2016) developed an acceleration feedback-based smart fuzzy controller for coastal bridge piers based on an MR damper and reported that the intelligent fuzzy controller effectively mitigated the impact response of the bridge pier-MR damper system under impact loading. Chen *et al.* (2018) used a TMD to control the seismic vibration of T-beam bridges with high-piers in the Sichuan-Tibet railway and noticed that the TMD can effectively control the seismic vibration of high piers by determining its best installation position and parameters. To prevent pier damage due to direct collisions between vehicles and ships, Hoang *et al*. (2016) developed a novel TMD system and applied it to a pier. It was found that the proposed TMD system had a better damage control effect than existing TMD systems. Relevant research on the foundation of piers and pier bearings also has been carried out to achieve superior pier vibration control. Chen and Li (2020) investigated the effectiveness of VDs in improving the seismic performance of a high pier bridge with a rocking foundation, and the results of the nonlinear time history analysis revealed that the VDs could effectively suppress the inclined seismic response of the rocking interface.

Yi *et al*. (2020) analyzed the potential of viscous

Correspondence to: Yuan Bo, Space Structures Research Center, Guizhou University, Guiyang 550004, China
Tel: +86-18798791201
E-mail: 313597338@qq.com
†PhD Candidate; ‡Professor
Received April 9, 2021; **Accepted** April 11, 2022

fluid dampers (VFDs) in suppressing bearing uplift caused by earthquakes and found that the VFDs slightly reduced the pounding force while effectively controlling the uplift displacement of the deck end. Li *et al*. (2016) designed a magnetorheological elastomeric bearing (MRB) with adjustable stiffness and damping parameters and reported that the isolation performance of the MRB was similar to that of traditional rubber bearings, which ensure the safety of bridges during earthquakes. Although previous studies have extensively investigated the energy dissipation and damping of bridge piers, less attention has been paid to the transverse energy dissipation and damping of double-column piers during earthquakes (Niu *et al.*, 2020). Hence, the lateral energy dissipation of double-column bridge piers has been investigated in detail in the current work.

This study presented a novel swing column device (SCD) based on an MR damper and designed a current controller to generate control currents for a double-column bridge pier with the SCD. According to the modeling method proposed by Seto (Seto and Mitsuta, 1994; Seto *et al.*, 1998), a lumped mass model for the double-column bridge pier with the SCD was established. Furthermore, a current controller based on fuzzy logic control was designed to determine control currents for the SCD. Finally, the motion equation of the double-column bridge pier with the SCD was established according to the D′Alembert principle and solved by computational programming.

2 Double-column bridge pier model

2.1 Double-column bridge pier model with SCD

The model of the double-column bridge pier with the SCD is shown in Fig. 1, and it is composed of a cover beam, a chute, two columns, a swing column, a fixed platform, a current controller, bolts, rollers, and an MR damper. The swing column in the SCD could move to the left and right along the chute, and the lower end of the swing column was fixed on the fixed platform and could rotate freely. The MR damper was installed at the vibration node of the two columns (vibration node is the point where the modal value is zero (Seto and Mitsuta, 1994)).

When an earthquake occurs, the lateral displacement of a pendulum column becomes unsynchronized with that of a double-column bridge pier. The current controller receives the displacement value transmitted by the sensor that is installed on the cover beam and the acceleration value transmitted by the sensor installed on the foundation. The current controller drives the SCD to generate the control force according to the obtained acceleration and displacement values and fuzzy set rules. The control flowchart of the SCD is shown in Fig. 2.

2.2 Simplified calculation model of the double-column bridge pier with the SCD

To analyze the vibration reduction performance of

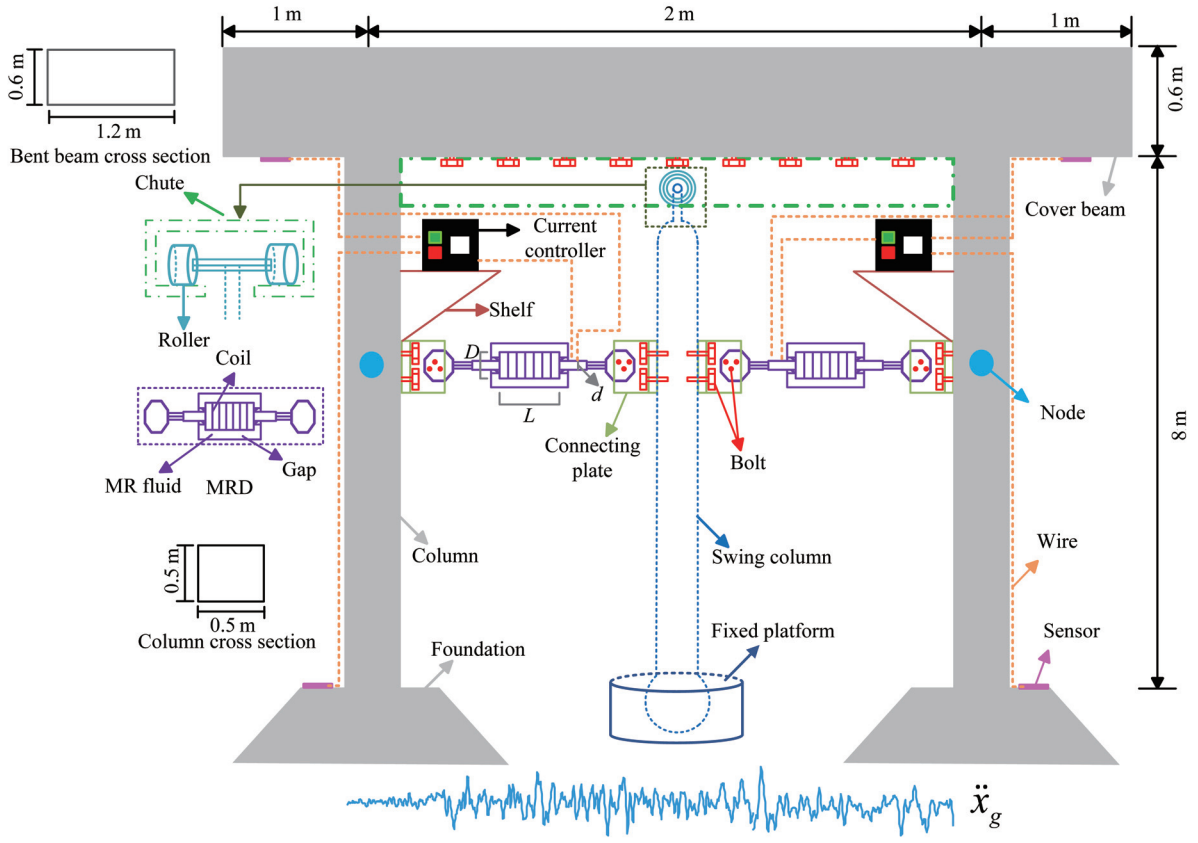

Fig. 1 Model of the double-column bridge pier with SCD

the SCD, a lumped mass model for the double-column bridge pier was established according to the low order modeling method proposed by Seto (Seto and Mitsuta, 1994; Seto *et al.*, 1998). The vibration mode shapes of flexible structures were first controlled, and the first to fifth modes of the double-column bridge pier were obtained by using finite element analysis (Fig. 3). The mode order was then determined to produce a lumped parameter system. Nodes of the lowest-order uncontrolled vibration mode were determined and used as setting points for the sensors (the fifth mode shape is shown in Fig. 3(e)). Subsequently, masses of the lumped parameter system were placed at the selected nodes to create a four-degrees-of-freedom system (Fig. 4). Finally, in the double-column bridge pier with the SCD, the swing column was separately concentrated into a particle (m_5, in Fig. 5).

The governing equation of the double-column bridge pier with the SCD can be expressed as:

$$\boldsymbol{M}\ddot{\boldsymbol{x}}(t)+\boldsymbol{C}\dot{\boldsymbol{x}}(t)+\boldsymbol{K}\boldsymbol{x}(t)=-\boldsymbol{M}\boldsymbol{I}_1\ddot{\boldsymbol{x}}_g+\boldsymbol{B}\boldsymbol{f}_d(t) \tag{1}$$

where $\boldsymbol{M}$ is the physical mass matrix, $\boldsymbol{C}$ is the physical damping matrix, $\boldsymbol{K}$ is the physical stiffness matrix, $\ddot{\boldsymbol{x}}(t)$ is the acceleration vector, $\dot{\boldsymbol{x}}(t)$ is the velocity vector, $\boldsymbol{x}(t)$ is the displacement vector, $\ddot{\boldsymbol{x}}_g$ is earthquake acceleration, $\boldsymbol{I}_1$ is the position vector of seismic waves, $\boldsymbol{B}$ is the position matrix of the SCD, and $\boldsymbol{f}_d(t)$ is the control force vector of the SCD.

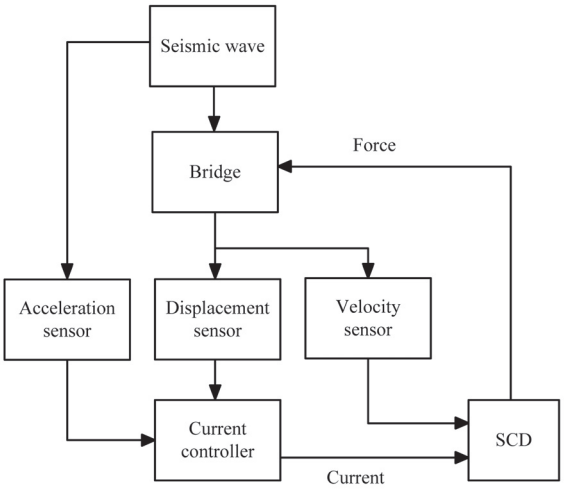

Fig. 2 Control flowchart of the SCD

$$\boldsymbol{M}=\begin{bmatrix} m_1 & & & & \\ & m_2 & & & \\ & & m_3 & & \\ & & & m_4 & \\ & & & & m_5 \end{bmatrix} \tag{2}$$

$$\boldsymbol{K}=\begin{bmatrix} \sum_{i=1}^{4}k_{1i} & -k_{12} & -k_{13} & -k_{14} & 0 \\ -k_{21} & \sum_{i=1}^{4}k_{2i} & -k_{23} & -k_{24} & 0 \\ -k_{31} & -k_{32} & \sum_{i=1}^{4}k_{3i} & -k_{34} & 0 \\ -k_{41} & -k_{42} & -k_{43} & \sum_{i=1}^{4}k_{4i} & 0 \\ 0 & 0 & 0 & 0 & k_{55} \end{bmatrix} \tag{3}$$

$$\boldsymbol{C}=\begin{bmatrix} \sum_{i=1}^{4}c_{1i} & -c_{12} & -c_{13} & -c_{14} & 0 \\ -c_{21} & \sum_{i=1}^{4}c_{2i} & -c_{23} & -c_{24} & 0 \\ -c_{31} & -c_{32} & \sum_{i=1}^{4}c_{3i} & -c_{34} & 0 \\ -c_{41} & -c_{42} & -c_{43} & \sum_{i=1}^{4}c_{4i} & 0 \\ 0 & 0 & 0 & 0 & c_{55} \end{bmatrix} \tag{4}$$

$$\ddot{\boldsymbol{x}}(t)=\begin{bmatrix}\ddot{x}_1\\ \ddot{x}_2\\ \ddot{x}_3\\ \ddot{x}_4\\ \ddot{x}_5\end{bmatrix},\quad \dot{\boldsymbol{x}}(t)=\begin{bmatrix}\dot{x}_1\\ \dot{x}_2\\ \dot{x}_3\\ \dot{x}_4\\ \dot{x}_5\end{bmatrix},\quad \boldsymbol{x}(t)=\begin{bmatrix}x_1\\ x_2\\ x_3\\ x_4\\ x_5\end{bmatrix} \tag{5}$$

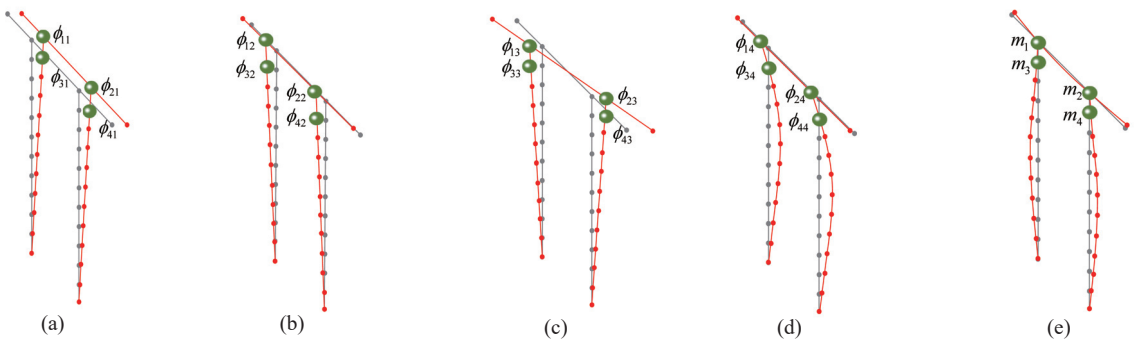

Fig. 3 Vibration modal diagram of the double-column bridge pier: (a) first-order mode (3.25 Hz), (b) second-order mode (5.82 Hz), (c) third-order mode (10.43 Hz), (d) fourth-order mode (29.29 Hz), and (e) fifth-order mode (38.1 Hz)

$$\boldsymbol{B}=\begin{bmatrix}0&0&0&0&0\\0&0&0&0&0\\0&0&1&0&0\\0&0&0&1&0\\0&0&1&-1&0\end{bmatrix},\quad \boldsymbol{I}_1=\begin{bmatrix}1\\1\\1\\1\\1\end{bmatrix},\quad \boldsymbol{f}_{\mathrm{d}}(\mathrm{t})=\begin{bmatrix}0\\0\\f_{\mathrm{d1}}\\f_{\mathrm{d2}}\\0\end{bmatrix} \tag{6}$$

where m_i is the ith mass, x_i is the displacement of mass i, $\dot{x}_i$ is the velocity of mass i, $\ddot{x}_i$ is the acceleration of mass i, k_{ij} is the spring constant between the ith mass and the jth mass, k_{ii} is the stiffness of the spring connecting the ith mass to the ground, c_{ij} is the damping constant between the ith mass and the jth mass, c_{ii} is the damping constant of the damper connecting the ith mass to the ground, and $f_{\mathrm{d}i}$ is the control force produced by the SCD (the value of i and j ranged from 1 to 5).

3 MR damper

The MR dampers are vibration-damping devices that are manufactured by exploiting the rapid and reversible rheological characteristics of MR fluids under a strong magnetic field (Rahman *et al.*, 2017; Wang and Liao, 2011). The performance of MR dampers is affected by numerous factors, such as magnetic field, magnetized particles, temperature, and stabilizer. Since 1995, the MR fluid developed by the Lord Corporation has attracted considerable attention. An MR damper is mainly composed of a coil, a cylinder, a piston, and an MR fluid. The function of an MR damper can be categorized into three modes (Rahman *et al.*, 2017): valve, direct shear, and squeeze (Moon *et al.*, 2011). To describe the mechanical properties of MR dampers, different models, such as the Bingham model, the Bouc-Wen model, the modified Bouc-Wen model, the equivalent viscous damping model, and the extended Bingham model, have been proposed (Azar *et al.*, 2020; Rahman *et al.*, 2019; Xu and Guo, 2008). In the present analysis, the extended Bingham model is used to represent the mathematical model of the MR damper because it is simple and can better simulate changes in damping force. The force-displacement relationship of the MR damper can be expressed as (Phillips, 1969):

$$f_{\mathrm{d}}=\frac{3LA_{\mathrm{p}}\tau_{\mathrm{y}}}{h}\mathrm{sgn}(u)+\frac{12\eta LA_{\mathrm{p}}^2}{\pi Dh^3}u \tag{7}$$

$$\tau_{\mathrm{y}}=A_1e^{-I}+A_2\ln(I+e)+A_3I \tag{8}$$

where η is the dynamic viscosity coefficient, L is the length of the piston; D is the inner diameter of the cylinder; h is the clearance of the cylinder; $A_{\mathrm{p}}=\pi(D^2-d^2)/4$ is the effective area of the piston; d is the piston diameter of the shaft; $\dot{u}$ is the piston velocity relative to the cylinder; sgn is a symbolic function; τ_{y} is the shear yield stress; I is the current; and A_1, A_2, and A_3 are the performance coefficients of the MR damper.

4 Design of the current controller based on fuzzy logic

The control efficiency of the extended Bingham model was mainly determined by use of the input current. A fuzzy logic algorithm was used to adjust the input current of the MR damper and control the output of the damper. The design process of the current controller is described below.

First, control parameters were selected. When vibration control meets comfort requirements, the acceleration response of a structure should be selected as a control variable. However, during an earthquake, structural safety is the most concerning issue; hence, the displacement response of structure also should be selected as a control variable. In the present analysis,

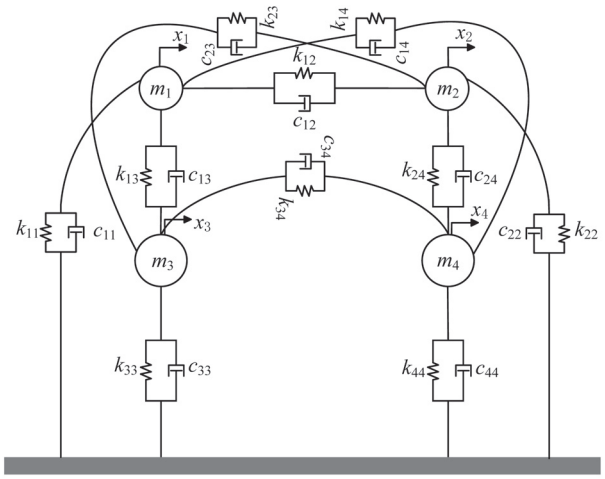

Fig. 4 Concentrated mass diagram of the double-column bridge pier

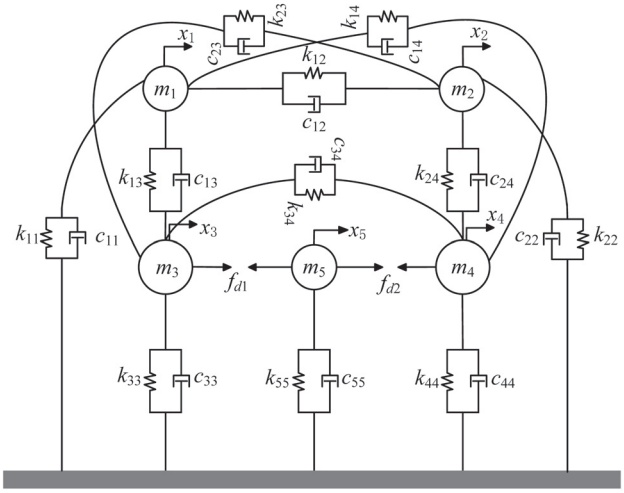

Fig. 5 Concentrated mass diagram of the double-column bridge pier with the SCD

the input to the controller is seismic acceleration and displacement response of the cover beam. The influence of a time delay can be weakened by inputting seismic information into the controller to generate a control force in advance, and the displacement input controller of the pier can solve the overshoot phenomenon.

Second, the selected parameters were fuzzified. After the selection of control parameters, the fuzzy domains of displacement and acceleration are determined according to the safety limit of a structure and the seismic intensity level of the area where the structure is located. The fuzzy domain of the input current is determined according to the current parameters of an MR damper. In the present analysis, earthquake acceleration and displacement of the cover beam are divided into five grades: positive small (PS), small (S), medium (M), big (B), and positive big (PB), and their membership function uses a triangular membership function. In an actual situation, the input to the current controller does not belong to the selected fuzzy domain. To avoid this situation, the acceleration quantization factor k_{acc}, the displacement quantization factor k_{dis}, and the current scale factor k_1 were used to adjust the range of input and output so that they belonged to their respective fuzzy domain.

Third, the extraction of the fuzzy rule was performed. When the response of earthquake acceleration and displacement was PS, the value of the control current was PS. When the response of earthquake acceleration and displacement was PB, the value of the control current was PB. Twenty-five control rules were obtained by analogy, and the rule table was adjusted locally according to the shock-absorption effect of the structure (Table 1).

Finally, defuzzification was carried out. Because it is simple and has a high degree of accuracy, the center of gravity method was selected to solve the fuzzy decision.

5 Simulation results and analysis

The dynamic response of the double-column bridge pier with the SCD during an earthquake was simulated. According to the theory proposed by Seto (Seto and Mitsuta, 1994; Seto *et al.*, 1998), the relevant parameters of the double-column bridge pier with the SCD were calculated. First, the modal matrix $\boldsymbol{\Phi}$ of the double-column bridge pier was obtained by using the finite element method (Eq. (9)). Second, the modified modal matrix $\overline{\boldsymbol{\Phi}}$ (Eq. (10)) was obtained by modifying the modal matrix $\boldsymbol{\Phi}$. The equivalent mass $\boldsymbol{M}_1$ and equivalent stiffness $\boldsymbol{K}_1$ of the double-column bridge pier were calculated by using Eqs. (11) and (12), respectively. Finally, the mass m_5 and the stiffness k_{55} were estimated by using an analogy to the actual column and subsequently confirmed according to the requirements of the control force. The parameters of the double-column bridge pier are listed in Table 2.

It should be noted here that the non-diagonal values of mass matrix $\boldsymbol{M}_1$ and stiffness matrix $\boldsymbol{K}_1$ are calculated by using $\overline{\boldsymbol{\Phi}}$, which is not zero. The non-diagonal values of mass matrix $\boldsymbol{M}_1$ and stiffness matrix $\boldsymbol{K}_1$ are calculated to be zero by using the modified modal matrix $\overline{\boldsymbol{\Phi}}$.

$$\boldsymbol{\Phi}=\begin{bmatrix}\phi_{11} & \phi_{12} & \phi_{13} & \phi_{14}\\ \phi_{21} & \phi_{22} & \phi_{23} & \phi_{24}\\ \phi_{31} & \phi_{32} & \phi_{33} & \phi_{34}\\ \phi_{41} & \phi_{42} & \phi_{43} & \phi_{44}\end{bmatrix}=\begin{bmatrix}0.0612 & 0.0577 & -0.0468 & -0.0233\\ 0.0612 & -0.0577 & -0.0468 & 0.0233\\ 0.0537 & 0.0599 & -0.0457 & 0.0088\\ 0.0537 & -0.0599 & -0.0457 & -0.0088\end{bmatrix} \tag{9}$$

$$\overline{\boldsymbol{\Phi}}=\begin{bmatrix}\overline{\phi}_{11} & \overline{\phi}_{12} & \overline{\phi}_{13} & \overline{\phi}_{14}\\ \overline{\phi}_{21} & \overline{\phi}_{22} & \overline{\phi}_{23} & \overline{\phi}_{24}\\ \overline{\phi}_{31} & \overline{\phi}_{32} & \overline{\phi}_{33} & \overline{\phi}_{34}\\ \overline{\phi}_{41} & \overline{\phi}_{42} & \overline{\phi}_{43} & \overline{\phi}_{44}\end{bmatrix}=\begin{bmatrix}0.0090 & 0.0111 & -0.0446 & 0.0392\\ 0.0090 & -0.0111 & -0.0446 & -0.0392\\ 0.0228 & 0.0222 & -0.0029 & -0.0080\\ 0.0228 & -0.0222 & -0.0029 & 0.0080\end{bmatrix} \tag{10}$$

$$\boldsymbol{M}_1=(\overline{\boldsymbol{\Phi}}\,\overline{\boldsymbol{\Phi}}^{\mathrm{T}})^{-1} \tag{11}$$

$$\boldsymbol{K}_1=(\overline{\boldsymbol{\Phi}}^{\mathrm{T}})^{-1}\boldsymbol{\Omega}^2\overline{\boldsymbol{\Phi}}^{-1} \tag{12}$$

where $\boldsymbol{\Omega}$ is the diagonal matrix of the natural frequency structure.

The structural damping matrix $\boldsymbol{C}$ was determined according to the use of Rayleigh damping. In this work, the damping matrix $\boldsymbol{C}$ shown in Eq. (4) was not used. Rayleigh damping was adopted because the damping coefficient c_{ij} between m_i and m_j was difficult to obtain, as follows:

$$\boldsymbol{C}=\alpha\boldsymbol{M}+\beta\boldsymbol{K} \tag{13}$$

where the Rayleigh parameters α and β were calculated using first two lower-order mode frequencies (ω_1 and ω_2).

Table 1 Fuzzy control rules

Displacement	Earthquake acceleration				
	PS	S	M	B	PB
PS	PS	S	M	B	PB
S	S	M	B	B	PB
M	M	B	B	PB	PB
B	B	B	PB	PB	PB
PB	PB	PB	PB	PB	PB

$$\alpha = \frac{2\omega_1\omega_2(\zeta_1\omega_2 - \zeta_2\omega_1)}{\omega_2^2 - \omega_1^2}$$
$$\beta = \frac{2(\zeta_2\omega_2 - \zeta_1\omega_1)}{\omega_2^2 - \omega_1^2} \quad (14)$$

where ω_1 and ω_2 are the first and second eigen-frequencies of the structure, respectively, according to the "Code for seismic design of urban bridges" (CJJ 166-2011) as utilized in China. The damping ratio of a building structure should be 0.05; hence, $\zeta_1 = = \zeta_2 = = 0.05$. The external excitations of the structure under three different seismic waves with a peak value of 0.4 g (4 m/s^2) are shown in Fig. 6.

The SCD design that was based on fuzzy control is referred to as fuzzy control. The displacement reduction rate (β_{Dis}) and the acceleration reduction rate (β_{Acc}) can be defined as:

$$\beta_{\text{Dis-S}} = \frac{\max(x_{\text{SCD}}) - \max(x_{\text{NO}})}{\max(x_{\text{NO}})},$$
$$\beta_{\text{Acc-S}} = \frac{\max(\ddot{x}_{\text{SCD}}) - \max(\ddot{x}_{\text{NO}})}{\max(\ddot{x}_{\text{NO}})} \quad (15)$$

$$\beta_{\text{Dis-F}} = \frac{\max(x_{\text{Fuzzy}}) - \max(x_{\text{NO}})}{\max(x_{\text{NO}})},$$
$$\beta_{\text{Acc-F}} = \frac{\max(\ddot{x}_{\text{Fuzzy}}) - \max(\ddot{x}_{\text{NO}})}{\max(\ddot{x}_{\text{NO}})} \quad (16)$$

where $\beta_{\text{Dis-S}}$ and $\beta_{\text{Acc-S}}$ are the displacement and acceleration reduction rates of the structure under the control of the SCD and x_{SCD} and $\ddot{x}_{\text{SCD}}$ are the displacement and acceleration under the control of the SCD. Additionally, x_{NO} and $\ddot{x}_{\text{NO}}$ are the displacement and acceleration of the structure without the control of the SCD; $\beta_{\text{Dis-F}}$ and $\beta_{\text{Acc-F}}$ are the displacement and acceleration reduction rates of the structure under fuzzy control, respectively; and x_{Fuzzy} and $\ddot{x}_{\text{Fuzzy}}$ are the displacement and acceleration under fuzzy control.

5.1 Shock absorption analysis of SCD

The MR damper acted as the energy-consuming component in the SCD. The experiment on the MR damper was carried out by Ou and Guan (1999). The MR fluid was developed by Fudan University, China (Xu *et al.*, 2003). The parameters of the MR damper are presented in Table 3.

The energy dissipation performance of the SCD was verified from two aspects. First, when I = 0 A, the performance of the SCD was only related to velocity. Hence, when an earthquake occurs, if a power supply fails the SCD could generate a control force according to the received velocity signal. Second, when I = 2 A, the SCD generated the maximum control force according to the input current and the received velocity signal.

When fuzzy control was not considered, according to Eq. (1), the time history curves of the displacement and acceleration of m_1 were obtained by computational programming. Figures 7 and 8 show the dynamic response time history curves of m_1 when I = 0 A and 2 A under the action of the Taft Lincoln School Earthquake.

Figures 9 and 10 shown the dynamic response time

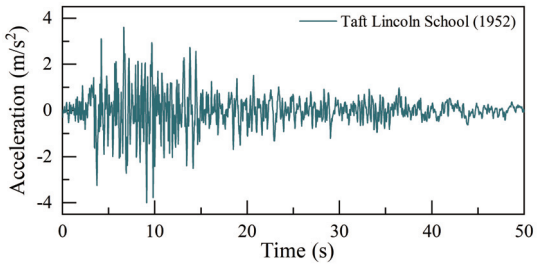

(a) Taft Lincoln School

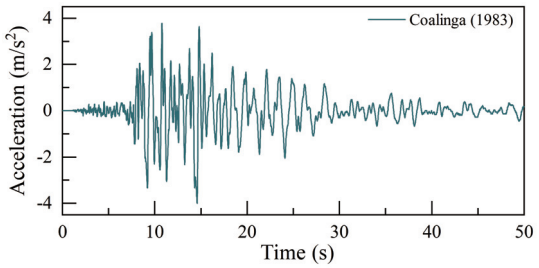

(b) Coalinga

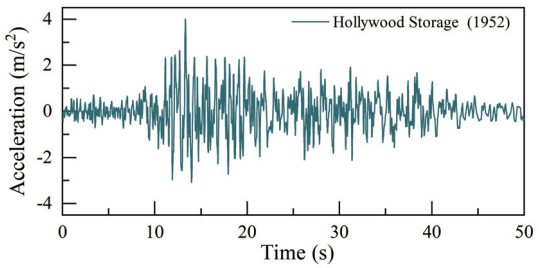

(c) Hollywood Storage

Fig. 6 Seismic waves

Table 2 Parameters of the double-column bridge pier with the SCD

Mass (kg)	Stiffness (N/m)
$m_1 = m_2 = 285.98$	$k_{11} = 6.61\times10^5$, $k_{12} = 4.19\times10^6$, $k_{13} = 2.49\times10^6$, $k_{14} = -2.02\times10^6$,
$m_3 = m_4 = 978.40$	$k_{22} = 6.61\times10^5$, $k_{23} = -2.02\times10^6$, $k_{24} = 2.49\times10^6$, $k_{33} = 1.14\times10^5$,
$m_5 = 2\times10^5$	$k_{34} = 1.14\times10^6$, $k_{44} = 1.14\times10^5$, $k_{55} = 2\times10^8$

Note: $k_{ij} = k_{ji}$ ($i = j = 1, 2\ldots$)

history curves of m_1 when I = 0 A and 2 A under the action of the Coalinga Earthquake.

Figures 11 and 12 shown the dynamic response time history curves of m_1 when I = 0 A and 2 A under the action of the Hollywood Storage Earthquake.

It is noticeable from Figs. 7, 9 and 11 that when the external power supply device of the SCD failed (I = 0 A), the SCD generated a control force according to the received velocity signal to the control structural vibration. At this time, the $\beta_{\text{Dis-S}}$ and $\beta_{\text{Acc-S}}$ of the double-column bridge pier with the SCD were –14.77% to –10.16% and –18.18% to –11.05%, respectively. When I = 2 A, the $\beta_{\text{Dis-F}}$ and $\beta_{\text{Acc-F}}$ of the double-column bridge pier with the SCD were –44.69% to –40.94% (Figs. 8(a), 10(a), 12(a)) and –6.12% to 29.09% (Figs. 8(b), 10(b), 12(b)), respectively.

Therefore, it can be inferred that the SCD device could effectively reduce the displacement of the pier. However, an overshoot occurred in the acceleration and local displacement of the pier because the SCD increased the stiffness and damping of the structure. Generally, with an increase in damping, the earthquake resistance of a structure is improved. However, with an increase in stiffness, more seismic energy is transferred to the structure. The seismic response of the bridge pier with the SCD were calculated by use of a time-history analysis. In this method, control forces were calculated according to the seismic responses of the bridge pier in previous epochs. Hence, control forces became distorted due to a time delay, causing an adverse effect on the control action. Furthermore, semi-active control has an inherent time delay. Therefore, to solve this problem, it is necessary to find an effective method that can control the future response of a structure in advance, as well as adjust feedbacks according to the actual responses of the structure to achieve the ideal state.

Therefore, two prominent problems were solved when SCD was used for the energy dissipative shock absorption of the double-column bridge pier. First, when the SCD directly generated a control force based on the current signal and the received structure velocity signal, it had a time delay. Thus, the SCD failed to generate an appropriate control force to protect the structure on time. Second, due to the relatively rough current input to the SCD, the controlled structure exhibited an acceleration overshoot under the influence of a small deformation.

Table 3 MR damper parameters

Piston length (L)	Inner diameter of cylinder (D)	Piston shaft diameter (d)	Cylinder clearance (h)	A_1	A_2	A_3	Coefficient (η)
400 mm	100 mm	40 mm	2 mm	–11374	14580	1281	0.9 Pa·m

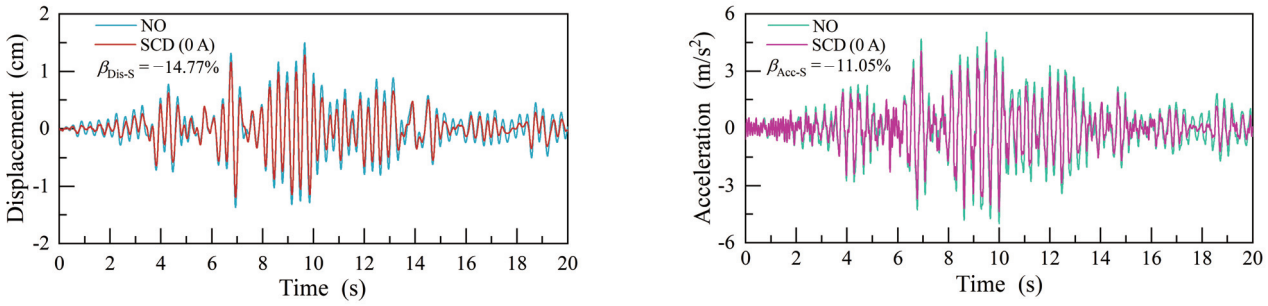

(a) Displacement (b) Acceleration

Fig. 7 Dynamic response time history curves of m_1 under the action of the Taft Lincoln School Earthquake at I = 0 A

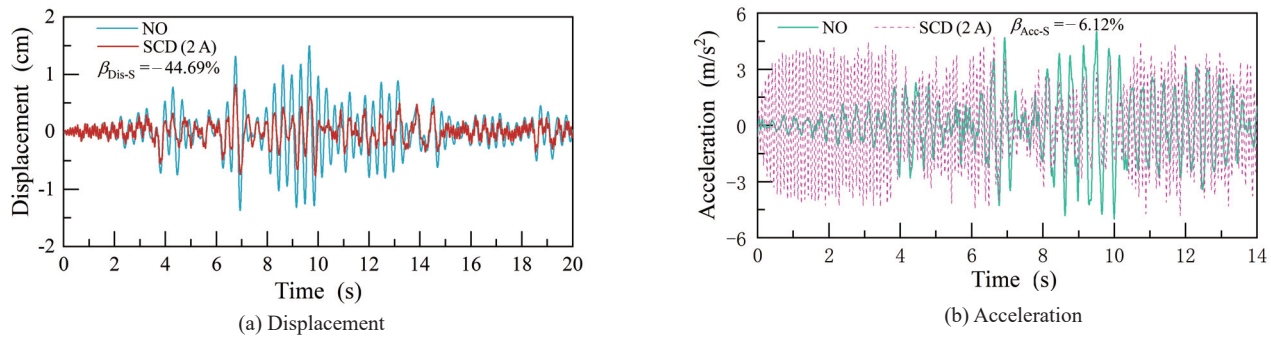

(a) Displacement (b) Acceleration

Fig. 8 Dynamic response time history curves of m_1 under the action of the Taft Lincoln School Earthquake at I = 2 A

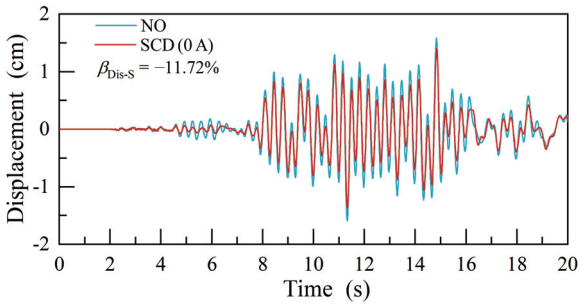

(a) Displacement

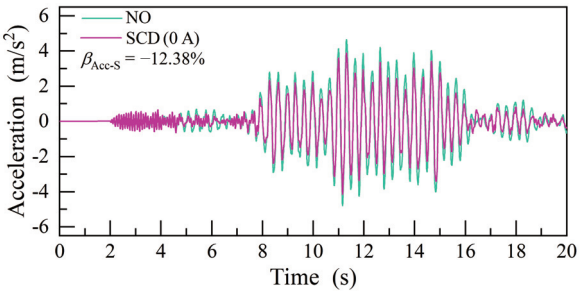

(b) Acceleration

Fig. 9 Dynamic response time history curves of m_1 under the action of the Coalinga Earthquake at I = 0 A

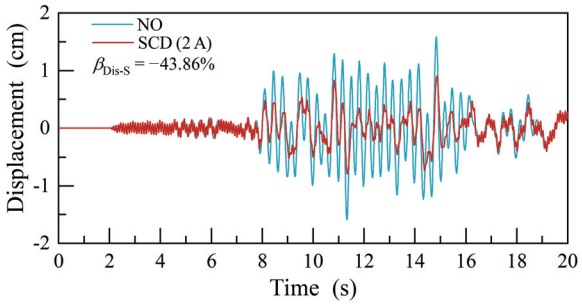

(a) Displacement

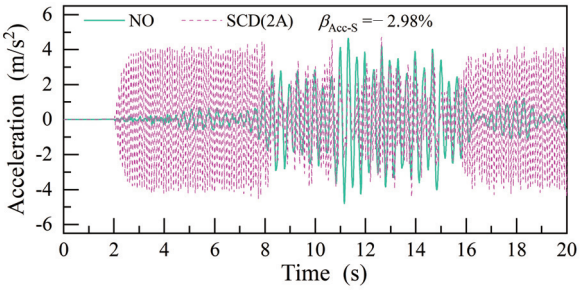

(b) Acceleration

Fig. 10 Dynamic response time history curves of m_1 under the action of the Coalinga Earthquake at I = 2 A

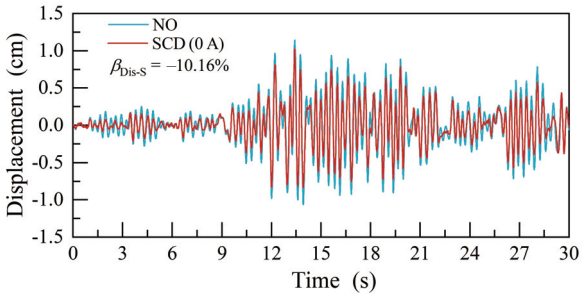

(a) Displacement

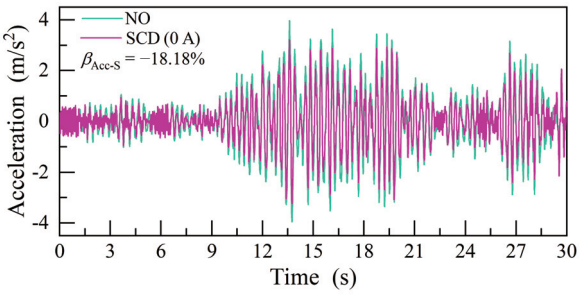

(b) Acceleration

Fig. 11 Dynamic response time history curves of m_1 under the action of the Hollywood Storage Earthquake at I = 0 A

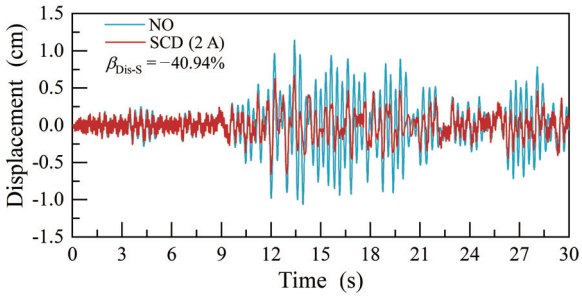

(a) Displacement

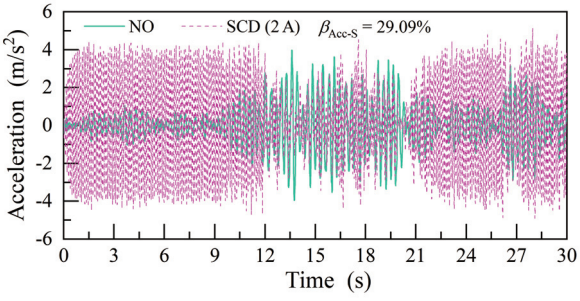

(b) Acceleration

Fig. 12 Dynamic response time history curves of m_1 under the action of the Hollywood Storage Earthquake at I = 2 A

5.2 Vibration reduction analysis of SCD based on fuzzy control

Fuzzy logic control has strong robustness and exhibits an accurate control parameter selection ability. It is considered the best method for solving time delay and current selection problems. In this work, to solve the aforementioned problems, a current controller based on the fuzzy logic control principle was designed. The controller included two inputs and one output. A seismic

wave was used as an input to the controller to weaken the time lag problem. The displacement of the structure was used as another input to the current controller to solve the overshoot problem.

To reduce the computing time of the controller, fuzzy domains used positive values. As the peak value of the seismic wave was 4 m/s^2, the fuzzy domain of acceleration was [0, 4]. To simplify the calculation, the upper limit of the fuzzy domain of displacement was set as the maximum value under the action of the three seismic waves. The fuzzy domain of displacement (Unit: m) was [0, 0.015], and the maximum displacement of m_1 was obtained according to the information listed Table 4. The output current amplitude of the controller was selected according to MR damper parameters. The maximum current input to the MR damper was 2 A; hence, the current fuzzy domain was [0, 2]. The corresponding membership function curves and surface views are plotted in Fig. 13. In an actual scenario, the fuzzy domain of acceleration can be selected according to seismic intensity and the nature of the construction project area. The fuzzy domain of displacement was selected according to the allowable displacement of the structure. The current fuzzy domain was selected

Table 4 Maximum dynamic responses of the double-column bridge pier

Working condition		Displacement (cm)				Acceleration (m/s^2)			
		No SCD	SCD		Fuzzy	No SCD	SCD		Fuzzy
			0 A	2 A			0 A	2 A	
Taft Lincoln School	m_1, m_2	1.4	1.27	0.82	0.88	5.14	4.58	4.83	3.6
	m_3, m_4	3.15	2.66	1.7	1.93	10.67	9.04	8.05	8.21
Coalinga	m_1, m_2	1.5	1.41	0.9	0.94	4.78	4.18	4.53	3.08
	m_3, m_4	3.4	2.97	1.89	2	10.08	8.64	5	5.74
Hollywood Storage	m_1, m_2	1.14	1.03	0.67	0.72	3.97	3.25	5.13	2.72
	m_3, m_4	2.46	2.19	1.35	1.50	9.03	7.47	4.86	5.11

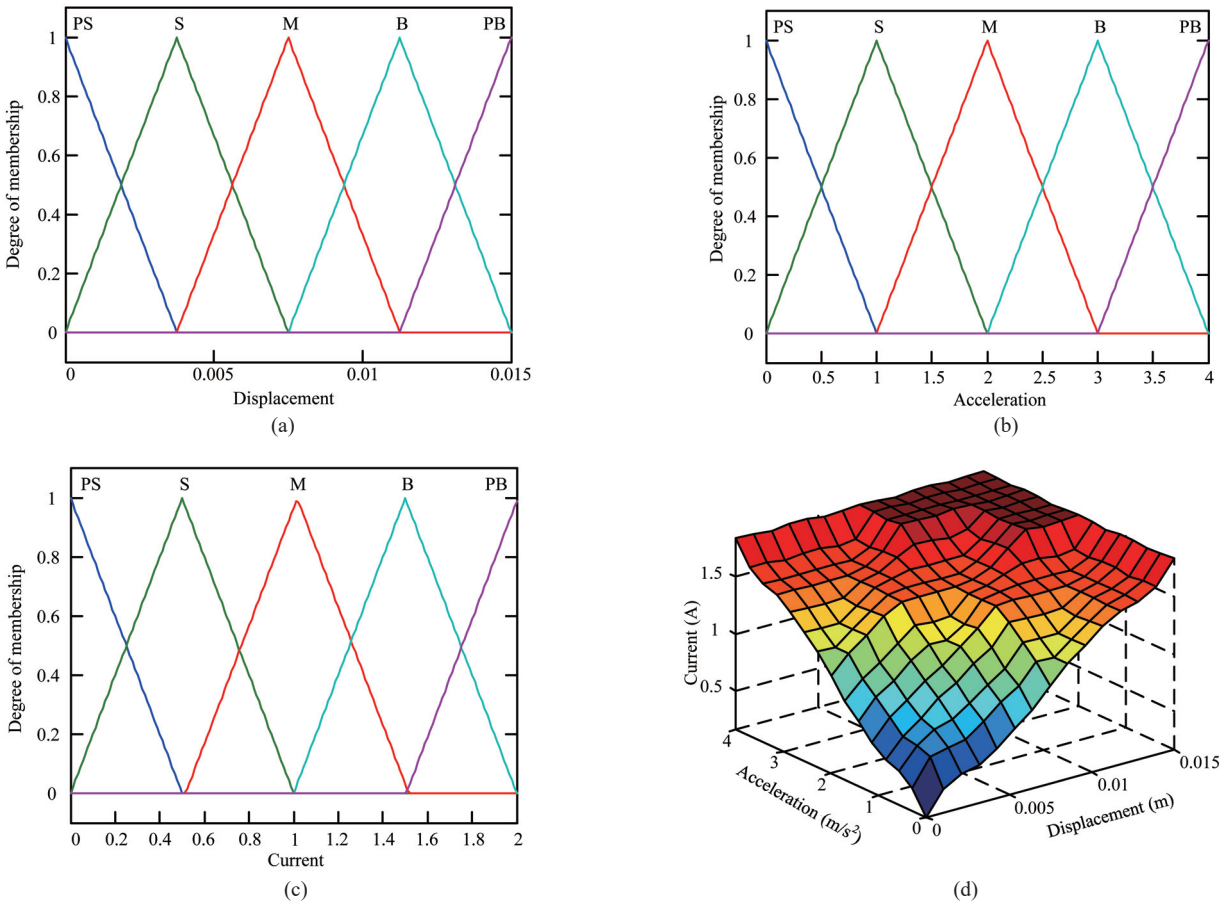

Fig. 13 Membership function curves of the current controller: (a) displacement, (b) acceleration, (c) current, and (d) surface view

according to MR damper parameters.

According to fuzzy control, Eq. (1) was recalculated and the displacement and acceleration time history curves of m_1 were re-plotted. Figures 14, 15, and 16 show the dynamic response time history of m_1 during the Taft Lincoln School Earthquake, the Coalinga Earthquake, and the Hollywood Storage Earthquake under fuzzy control. Table 4 presents the maximum dynamic responses of the double-column bridge pier under the influence of the three seismic waves.

It is evident from Figs. 14, 15, and 16 that fuzzy control effectively reduced the dynamic responses of the structure. The $\beta_{\text{Dis-F}}$ and $\beta_{\text{Acc-F}}$ were –40.63% to –36.43% and –33.6% to –30.06%, respectively, under fuzzy control, and no local overshoot of displacement was observed. A slight overshoot occurred in the local acceleration of the structure under fuzzy control. This slight local overshoot was not sufficient to affect the comfort of the structure; thus, it could be ignored.

It is clear from the information listed in Fig. 17 that the current controller outputs the appropriate current into the SCD according to received correlation information, and subsequently, the SCD generates the corresponding control force to obtain the ideal control effect (Figs. 14, 15, and 16). The control force produced under fuzzy control was smaller than that produced by the SCD when I = 2 A and was greater than that produced by the SCD when I = 0 A (Fig. 17). In comparison to SCD control, fuzzy control could generate the appropriate amount of control force in advance and weaken time delay and oscillation phenomena.

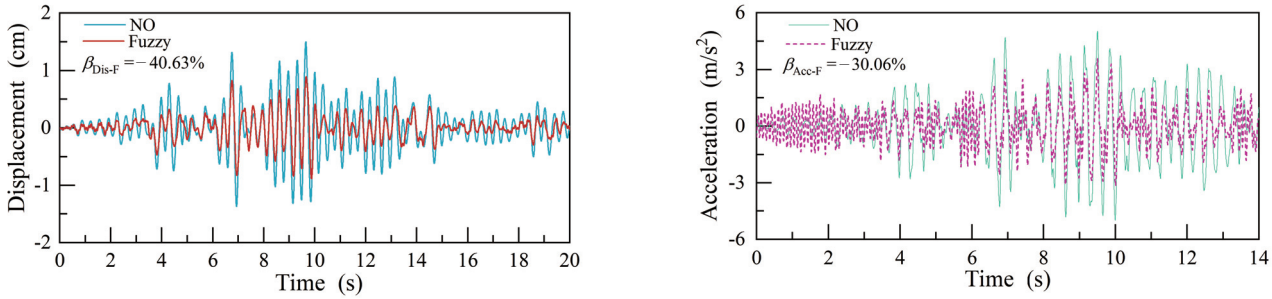

(a) Displacement (b) Acceleration

Fig. 14 Dynamic response time history curves of m_1 during the Taft Lincoln School Earthquake under fuzzy control

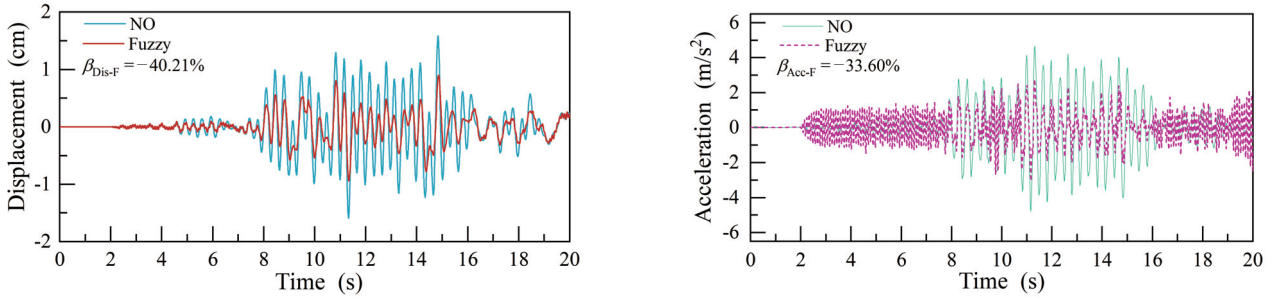

(a) Displacement (b) Acceleration

Fig. 15 Dynamic response time history curves of m_1 during the Coalinga Earthquake under fuzzy control

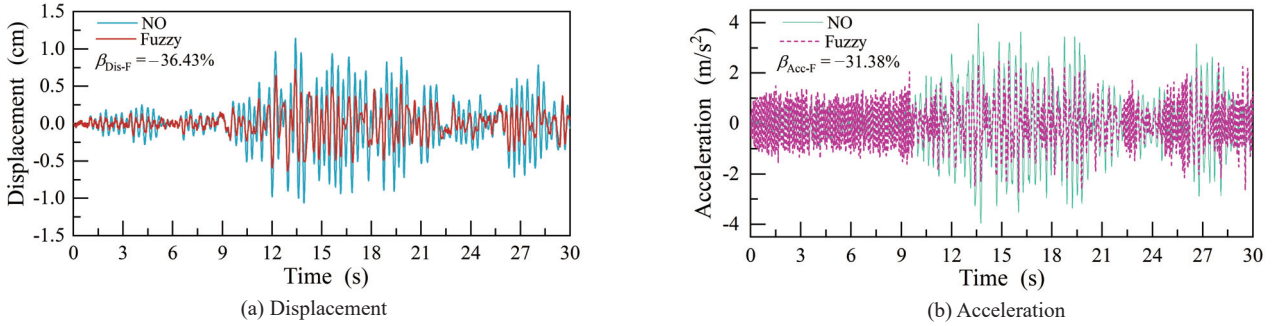

(a) Displacement (b) Acceleration

Fig. 16 Dynamic response time history curves of m_1 during the Hollywood Storage Earthquake under fuzzy control

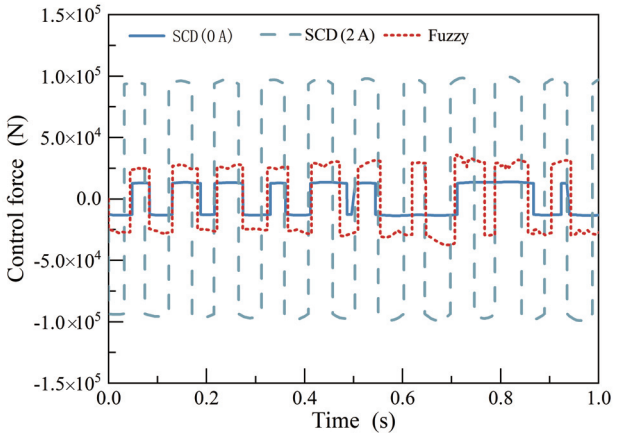

(a) Taft Lincoln School

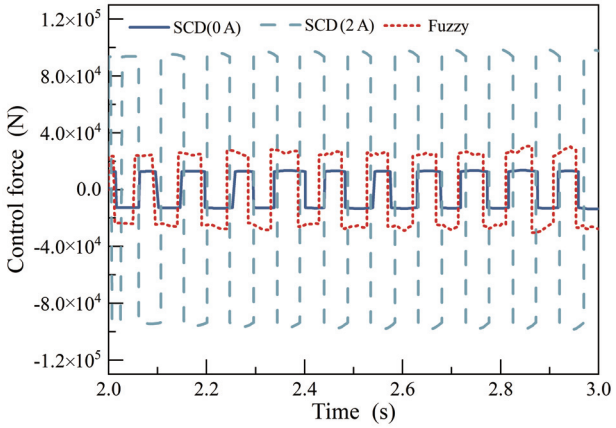

(b) Coalinga

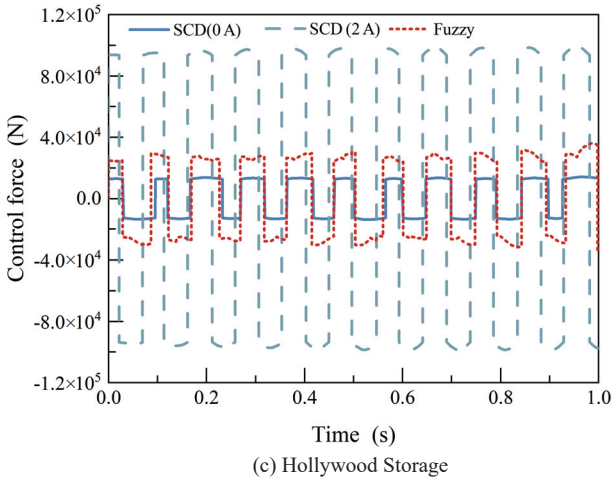

(c) Hollywood Storage

Fig. 17 Time history curves of the control force

6 Conclusion

To prevent the destruction of double-column bridge piers during earthquakes, a novel swing column energy dissipation device was designed. If the current device is applied directly to SCDs, the acceleration response of bridge structures increases greatly. Therefore, in order to solve this problem, a current controller was designed based on fuzzy logic control theory. According to the low-order modeling method proposed by Seto, the motion equation of the double-column bridge pier with the SCD was established and solved by computational programming. The main observations of this work are as follows:

(1) The novel SCD significantly reduced the dynamic response of the double-column bridge piers. Therefore, this device can be used as an effective energy dissipation tool to protect bridge structures from damages during earthquakes.

(2) The current controller design based on fuzzy logic theory quickly determined the appropriate current amplitude according to feedback information, without considering the precise mathematical model of the controlled object, thereby reflecting its superiority in practical applications.

(3) Although the fuzzy logic control theory weakened the excessive overshoot phenomenon, a slight overshoot was still noticed under external excitations. To eliminate this overshoot phenomenon, a neural network control algorithm can be used instead of the fuzzy logic control algorithm.

An elaborate experimental investigation on SCD will be carried out in future studies due to its advantages when employed in actual applications.

References

Arsava KS, Kim Y and Kim KH (2016),"Fuzzy Control for Impact Mitigation of Coastal Infrastructure Equipped with Magnetorheological Dampers," *Journal of Coastal Research*, **75**(SP1): 1037–1041.

Azar BF, Veladi H, Talatahari S and Raeesi F (2020), "Optimal Design of Magnetorheological Damper Based on Tuning Bouc-Wen Model Parameters Using Hybrid Algorithms," *Ksce Journal of Civil Engineering*, **24**(3): 867–878.

Chen X and Li CX (2020), "Seismic Assessment of Earthquake-Resilient Tall Pier Bridges Using Rocking Foundation Retrofitted with Various Energy Dissipation Devices," *Structural Control and Health Monitoring*, **27**(11): e2625.

Chen ZW, Han ZL, Zhai WM and Yang JZ (2018),"TMD Design for Seismic Vibration Control of High-Pier Bridges in Sichuan–Tibet Railway and Its Influence on Running Trains," *Vehicle System Dynamics*, **57**(2): 207–225.

Hoang T, Ducharme KT, Kim Y and Okumus P (2016), "Structural Impact Mitigation of Bridge Piers Using Tuned Mass Damper," *Engineering Structures*, **112**: 287–294.

Huang FY, Peng GZ and Wang XY (2019), "Study on Energy Dissipation of Viscous Damper for Long-Span Suspension Bridges," *Proceedings of the 5th International Conference on Environmental Science and Civil Engineering*, Vol. 283, Nanchang, China.

Jiang Z and Christenson RE (2012), "A Fully Dynamic Magneto-Rheological Fluid Damper Model," *Smart Materials and Structures*, **21**(6): 65002–65013(12).

Kahya V and Araz O (2020), "A Simple Design Method for Multiple Tuned Mass Dampers in Reduction of Excessive Vibrations of High-Speed Railway Bridges," *Journal of the Faculty of Engineering and Architecture of Gazi University*, **35**(2): 607–618.

Lavasani SHH, Alizadeh H, Doroudi R and Homami P (2020), "Vibration Control of Suspension Bridge due to Vertical Ground Motions," *Advances in Structural Engineering*, **23**(12): 2626–2641.

Li R, Li X, Wu YY, Chen SW and Wang XJ (2016), "Analysis of Longitudinal Seismic Response of Bridge with Magneto-Rheological Elastomeric Bearings," *Proceedings of the Conference on Sensors and Smart Structures Technologies for Civil, Mechanical, and Aerospace Systems*, Vol. 9803, Las Vegas, NV, USA.

Li X, Li J, Zhang XY, Gao JF and Zhang C (2020),"Simplified Analysis of Cable-Stayed Bridges with Longitudinal Viscous Dampers," *Engineering, Construction and Architectural Management*, **27**(8): 1993–2022.

Moon SJ, Huh YC, Jung HJ, Jang DD and Lee HJ (2011), "Sub-Optimal Design Procedure of Valve-Mode Magnetorheological Fluid Dampers for Structural Control," *KSCE Journal of Civil Engineering*, **15**(5): 867–873.

Niu JT, Ding Y, Shi YD and Li ZX (2020), "A Simplified Design Method for Metallic Dampers Used in the Transverse Direction of Cable-Stayed Bridges," *Earthquake Engineering and Engineering Vibration*, **19**(2): 483–497.

Ou JP and Guan XC (1999), "Experimental Study of Magnetorheological Damper Performance," *Earthquake Engineering and Engineering Vibration*, **19**(4): 76–81. (in Chinese)

Panji PS, Ilyas T and Bahsan E (2018), "Assessment of Bridge Substructure in Java Island," *Proceedings of the 3rd International Conference on Sustainable Infrastructure and Built Environment* (*SIBE*), Vol. 147, Inst Teknologi Bandung, Fac Civil & Environm Engn, Bandung, Indonesia.

Phillips RW (1969), *Engineering Applications of Fluids with a Variable Yield Stress*, University of California, Berkeley, USA.

Pozos-Estrada A, Garcia-Soto AD, Gomez R, Sanchez R and Escobar JA (2011), "Use of TMDs to Mitigate the Vibration of a Curved Steel Bridge," *Proceedings of the 8th International Conference on Structural Dynamics* (*EURODYN*), Leuven, Belgium, pp. 1124–1128.

Rahman M, Ong ZC, Chong WT and Julai S (2019),"Smart Semi-Active PID-ACO Control Strategy for Tower Vibration Reduction in Wind Turbines with MR Damper," *Earthquake Engineering and Engineering Vibration*, **18**(4): 887–902.

Rahman M, Ong ZC, Julai S, Ferdaus MM and Ahamed R (2017), "A Review of Advances in Magnetorheological Dampers: Their Design Optimization and Applications," *Journal of Zhejiang University-Science A*, **18**(12): 991–1010.

Seto K and Mitsuta S (1994), "A New Method for Making a Reduced-Order Model of Flexible Structures Using Unobservability and Uncontrollability and Its Application in Vibration Control," *JSME International Journal Ser C, Dynamics, Control, Robotics, Design And Manufacturing*, **37**(3): 444–449.

Seto K, Ren M and Doi F (1998), "Feedback Vibration Control of a Flexible Plate at Audio Frequencies by Using a Physical State-Space Approach," *The Journal of the Acoustical Society of America*, **103**(2): 924–934.

Wang DH and Liao WH (2011), "Magnetorheological Fluid Dampers: A Review of Parametric Modelling," *Smart Materials and Structures*, **20**(2): 023001.

Wang SY, Xiong ZH, Wang SL, Hu Y, Yang X and Chen PW (2020), "Analyzing and Modeling Post-Earthquake Emergency Traffic Demand," *Proceedings of the 13th Asia Pacific Transportation Development Conference - Resilience and Sustainable Transportation Systems*, Shanghai Univ Engn Sci, Shanghai, China, pp: 166–175.

Xie LL and Qu Z (2018), "On Civil Engineering Disasters and Their Mitigation," *Earthquake Engineering and Engineering Vibration*, **17**(1): 1–10.

Xu ZD and Guo YQ (2008), "Integrated Intelligent Control Analysis on Semi-Active Structures by Using Magnetorheological Dampers," *Science in China Series E: Technological Sciences*, **51**(12): 2280–2294.

Xu ZD, Jia DH and Zhang XC (2012),"Performance Tests and Mathematical Model Considering Magnetic Saturation for Magnetorheological Damper," *Journal of Intelligent Material Systems and Structures*, **23**(12): 1331–1349.

Xu ZD, Shen YP and Guo YQ (2003), "Semi-Active Control of Structures Incorporated with Magnetorheological Dampers Using Neural Networks," *Smart Materials and Structures*, **12**(1): 80–87.

Xu ZD, Xu M and Jia DH (2019), "Suppression of Vibrations Induced by Fluctuating Wind for Long-Span Cable-Stayed Bridge Using MR Dampers," *The International Journal of Acoustics and Vibration*, **24**(2): 262–270.

Yi J, Zhou JY and Ye XJ (2020), "Seismic Evaluation of Cable-Stayed Bridges Considering Bearing Uplift," *Soil Dynamics and Earthquake Engineering*, **133**: 106102.

Zhao YL, Xu ZD and Wang C (2019), "Wind Vibration Control of Stay Cables Using Magnetorheological Dampers Under Optimal Equivalent Control Algorithm," *Journal of Sound and Vibration*, **443**: 732–747.